International Journal of the Physical Sciences Vol. 5(11), pp. 1660-1670, 18 September, 2010
Available online at http://www.academicjournals.org/IJPS
ISSN 1992 - 1950 ©2010 Academic Journals

Full Length Research Paper

Out-of-plane seismic analysis of Bozdogan (Valens) aqueduct in Istanbul

M. Arif Gurel*, Kasim Yenigun and R. Kadir Pekgokgoz

Faculty of Engineering, Harran University, Civil Engineering Department, Osmanbey Campus, 63190, Sanliurfa, Turkey.

Accepted 17 September, 2010

The Bozdogan (Valens) aqueduct in Istanbul is one of the most prominent water supply structures inherited from the Byzantine period. The paper investigates the out-of-plane seismic resistance of the aqueduct. The structural system of the aqueduct is composed of a series of piers connected to each other with arches at two tier levels. Taking advantage of the structural periodicity, only one pier of the highest part of the aqueduct is considered for the analysis instead of the whole structure. This pier is modelled as a cantilever prismatic element subjected to gravity load and increasing lateral load representing out-of-plane seismic loading. It is assumed that the pier is made of a no-tension material, with a linear stress-strain relationship in compression, and has infinite compression strength. To accomplish the solution, an efficient numerical model and solution procedure developed by La Mendola and Papia for investigating the stability of masonry piers under their own weight and an eccentric top load, is utilised and adapted to the problem at hand. The analysis showed that, although, the aqueduct can withstand out-of-plane earthquake ground motions of medium size and usually encountered periods, it is vulnerable to the ones containing long-period pulses.

Key words: Bozdogan (Valens) aqueduct, seismic, out-of-plane resistance, numerical model.

INTRODUCTION

Istanbul is one of the most ancient and wonderful cities of the world. It had been the capital of two world empires; Byzantine (Eastern Roman) and Ottoman Empires. These empires left such a large and varied construction heritage that the city can be regarded as an open-air museum. Almost all of these heritages had been realized with masonry material.

Unfortunately, Istanbul is located in a seismically active region. As proven by historical sources, the city has been subjected to many destructive earthquakes in its history (Ambraseys and Finkel, 1990, 1995; Barka, 2000; Eyidogan, 2000). Many structures were seriously damaged and many others completely collapsed during the earthquakes. Today also, the city is under the threat of imminent great earthquakes. On the other hand; water, undoubtedly has a vital importance for life. Human being has spent great efforts for transporting water to the place where he lived and settled throughout the history. For this aim, man has built various magnificent water structures such as dams, tunnels, channels, aqueducts etc. It can be given the Pont du Gard in France (Panoramio, 2009), Segovia in Spain (Wikimedia, 2009) and Moglova in Istanbul - Turkey (TCF, 2009) samples for the aqueducts, Figure 1.

Istanbul also comprises many aqueducts in its historical structure stock. Most of them were constructed during the Roman and Ottoman periods. For example, the Bozdogan aqueduct is one of these utility structures and an important part of the ancient water conveyance system of the city. This system has approximately 242 km length and originates from the Istranca (Thrace) Springs and ends at the Yerebatan (Basilica) Cistern at Sultanahmet Square (Cecen, 1996). According to Cecen (1996) the discharge of the Istranca Springs varied between 0.3 - 1.0 m^3/s. It is generally assumed that the aqueduct was built during the reign of the Roman

*Corresponding author. E-mail: agurel@harran.edu.tr, a_gurel@hotmail.com. Tel: + 90(414)3183777. Fax: +90(414)3183799.

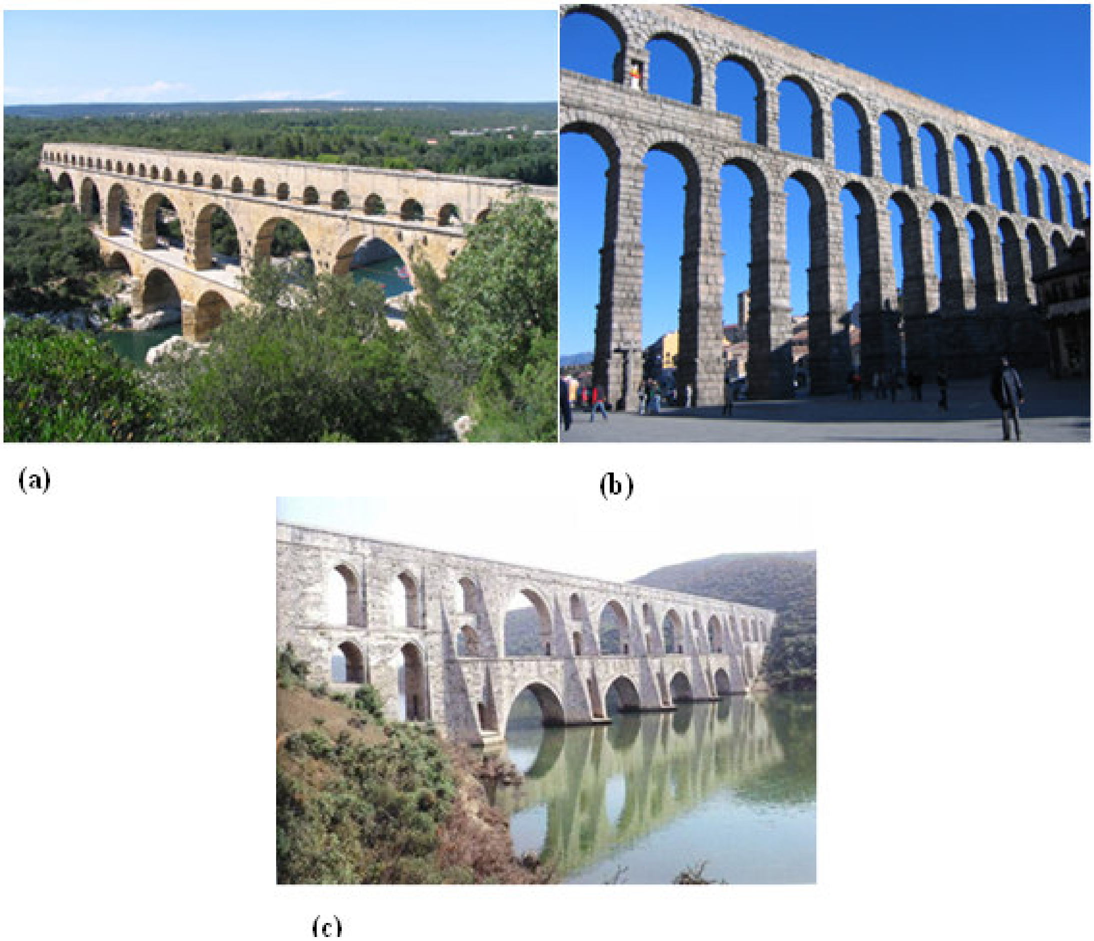

Figure 1. Three magnificent aqueducts: (a) Pont du Gard, France (Panoramio, 2009) (b) Segovia, Spain (Wikimedia, 2009) and (c) Moglova, Istanbul (TCF, 2009).

Emperor Valens (A.C. 364-378); so the structure is also called the Valens aqueduct (Eyice, 1992; Yorulmaz and Celik, 1995). The location of the structure in the city and it’s a typical part are shown in Figures 2 and 3, respectively. The structural system of the aqueduct is composed of a series of piers connected to each other with arches at two tier levels. Although, the original total length of this stone masonry structure is estimated at about 970 meters, only a part of it exists today (Akinci, 1992; Yorulmaz and Celik, 1995).

It has been restored many times since the Byzantine period. The main causes of damage and collapse were attacks during occupations of the city and strong earthquakes over the course of time. For the last restoration project in 1988 it had to be checked under gravity loading, because it was necessary to open some of the infilled arches at ground level. This check was done by Yorulmaz and Celik (1995) using a numerical calculation procedure and it was seen that almost all maximum stresses are within the acceptible limits for the structure.

As mentioned above, the structure was damaged and some parts of it collapsed due to strong earthquakes that occured in the past. For example, it is generally considered that its missing part at the Beyazit Square side was destroyed by the devastating earthquake in 1509 (Akinci, 1992; Yorulmaz and Celik, 1995). For the protection of such a splendid and irreplaceable historical structure from the demolishing influences of possible earthquakes in future, first of all its resistance against earthquakes must be determined. So far, to the authors’ best knowledge, any study about earthquake resistance of this structure has not been carried out. Today, the structure straddles one of the major highways of the city, Figure 3.

It can be said that, the most unfavorable loading condition occurs when the earthquake ground motion is directed orthogonally (out-of-plane) to the plane of such a high and wall type structure. There is a possibility of overturning due to inertia forces in this direction during a large earthquake. It is well documented that inadequate resistance against out-of-plane seismic forces is one of

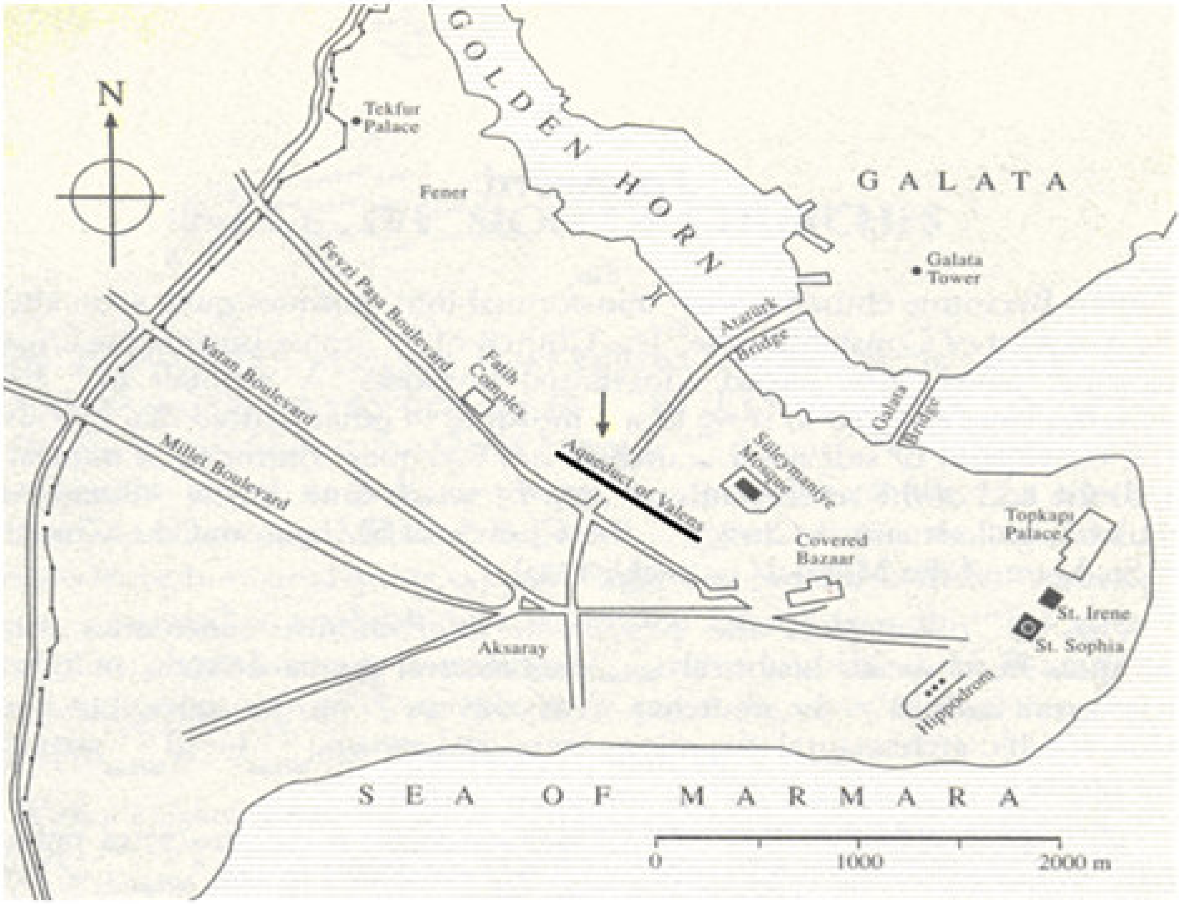

Figure 2. Location of the Bozdogan (Valens) aqueduct in the historical peninsula of Istanbul (Kirimtayif, 2001).

Figure 3. A general view of the Bozdogan (Valens) aqueduct (by authors).

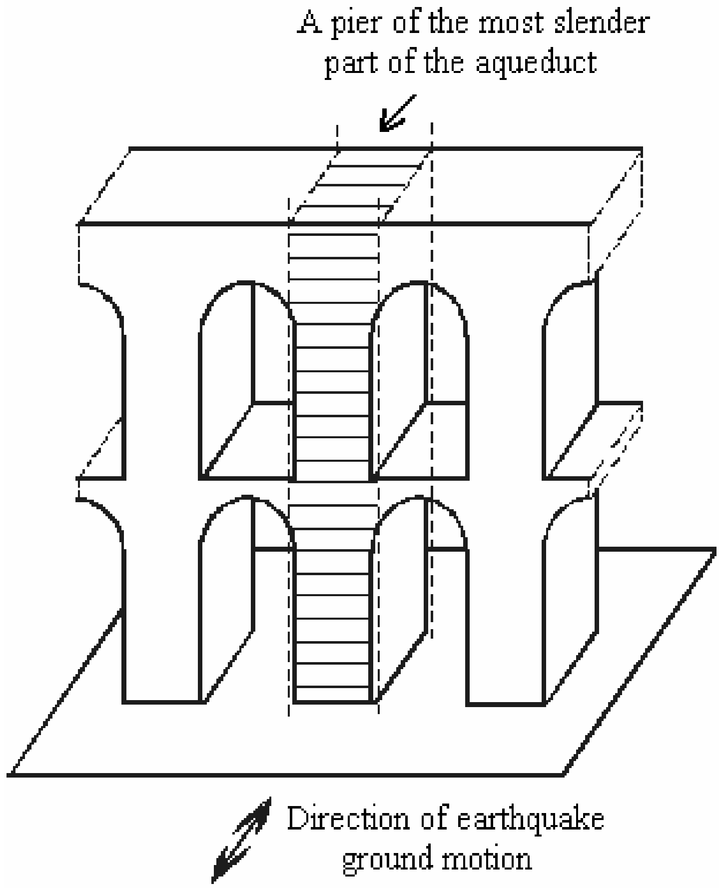

Figure 4. Pier considered for determining out-of-plane seismic resistance of the aqueduct.

the primary causes of damage and collapse of many masonry structures during earthquakes (Bruneau and Lamontagne, 1994; Fardis, 1995; Casolo, 2000; De Felice and Giannini, 2001). Therefore, in this study, it is aimed to determine the out-of-plane seismic resistance of this historical structure. Thus, the obtained findings can also be useful for any intervention, which may be required, for the strengthening of the structure.

For the analysis, a numerical model developed by La Mendola and Papia (1993) for investigating the stability of masonry piers under their own weight and an eccentric top load is utilised and adapted to the problem. The model takes into account the cracking of the sections and the second-order effects.

ANALYSIS MODEL

As it is known, there are three levels of analysis of structures under lateral seismic effects. These are; dynamic time-history analysis, modal superposition analysis and equivalent static analysis. One can find detailed information about these analysis methods, for example, in Paulay and Priestly (1992). Here, for the out-of-plane seismic analysis of the aqueduct, due mainly to its simplicity, the equivalent static lateral load analysis is preferred. Since this analysis procedure takes only into account the fundamental vibration mode of the structure and ignores the consideration of higher modes, it adopts an inverted triangular static lateral load distribution along the height of the structure, equivalent to the maximum inertia effects. Therefore, in here, analysis is performed on the most slender part which is considered as the most vulnerable part of the aqueduct under out-of-plane seismic effects. This part of the structure, Figure 3, may be considered as a succession of identical piers subjected to the same loading conditions. Hence, interaction forces such as moments and shear forces between piers can be neglected. Moreover, buttresses at both sides of the piers can also be neglected, because only a small portion of them are above the ground level at the present condition. Therefore, in order to determine out-of-plane seismic resistance of the aqueduct, instead of the whole structure, only one pier of the most slender part can be considered, Figure 4. The pier can be taken as a prismatic element fixed at its base and free at the top. Figure 5a shows a fixed-free ended masonry pier of width B, depth D and height H. The pier is ideally divided into n finite elements, all having the same height $H_e = H/n$, numbered from 1 to n, starting from the top end and restricted by n+1 sections, numbered from 0 to n (La Mendola and Papia, 1993; La Mendola et al., 1995), Figure 5b. W and W/n indicate total weight of the pier and weight of the each element, respectively. Lateral seismic loading, assumed to be acting statically, consists of an increasing horizontal inertia force f_j proportional to the weight W/n and to the location of the point of

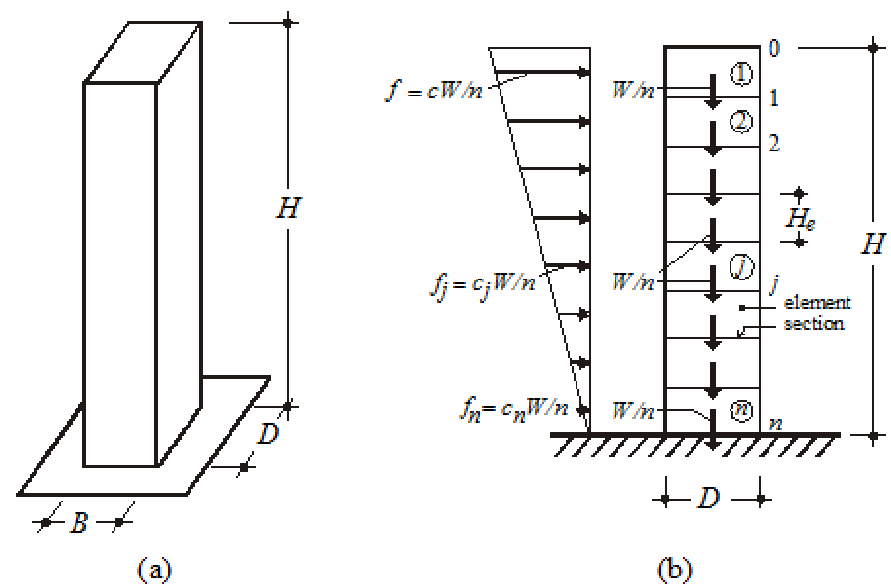

Figure 5. (a) Geometry of a pier and (b) Its discretized model and loading condition.

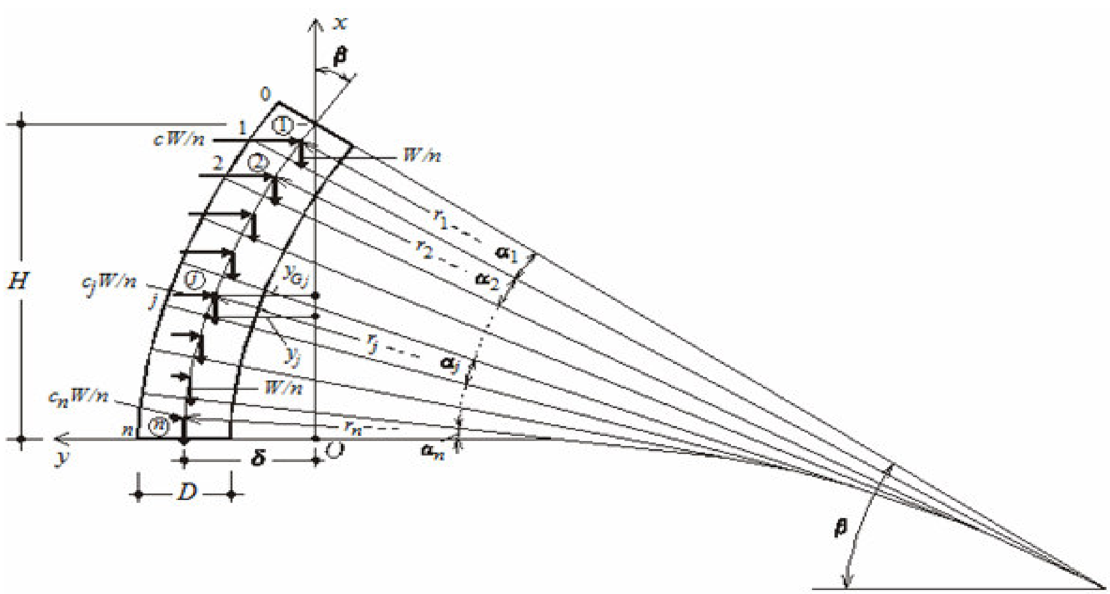

Figure 6. Deformed shape of the pier under considered loading condition.

application, that is,

$$f_j = c_j \frac{W}{n} = c[(n - j + 1/2)/(n - 1/2)]\frac{W}{n} \qquad (1)$$

Where c will be defined as seismic coefficient describing the intensity of the earthquake loading. Each element is affected by the weight W/n and the inertia force c_jW/n. Both these forces are assumed to be concentrated and applied to the center of mass of the element. Equation (1) defines an inverted triangular lateral loading and the response of the pier to this loading is approximately proportional to the first vibration mode. Thus, the loading allows to identify the collapse mode of the pier and also to evaluate the maximum intensity c_{max} of the out-of-plane response of the structure (La Mendola et al., 1995; Pegon et al., 2001).

The highly magnified deformed shape of the pier under considered loading condition is shown in Figure 6. The curvature of each element is assumed as constant and defined by the value at its upper section. When the dimensionless height of the elements (the discretization parameter) defined by $\xi = H_e/D = H/nD$ is small enough, namely, the number n is sufficiently high, this approximation is well founded (La Mendola et al., 1995).

The numerical model can be used to deduce the whole $c-\delta$ curve and c_{max} for this masonry pier, using dimensionless parameters explained in the following. Using the notations in Figure 6, the coordinate y of the jth cross section can be written as

$$y_j = y_{j-1} + r_j\left[\cos\left(\beta-\sum_{i=1}^{j}\alpha_i\right)-\cos\left(\beta-\sum_{i=1}^{j-1}\alpha_i\right)\right] \quad (2)$$

(j = 1, 2, ..., n)

Where β is the rotation of the top cross-section, r_j is the radius of curvature of the jth element and $\alpha_j = H_e/r_j$ is the angle related to it in the discretized model (La Mendola and Papia, 1993; La Mendola et al., 1995). Expanding the cosine function in the Taylor's series and taking first three terms only, Equation (2), in dimensionless form, becomes

$$\frac{y_j}{D} = \frac{y_{j-1}}{D} + \xi\beta + \frac{1}{2}\xi^2\phi_j D - \sum_{i=1}^{j}\xi^2\phi_i D \quad (3)$$

(j = 1, 2, ..., n)

Where $\phi_i = 1/r_i$ is the curvature of the ith element (La Mendola and Papia, 1993; La Mendola et al., 1995).

Since y_0 = 0, Figure 6, and when ξ is selected, one can obtain the deformed shape of the pier, corresponding to the top section rotation β, by using Equation (3) recursively, starting from the index j = 1. But this can only be done, if the curvatures of all the elements are also known (La Mendola et al., 1995).

Assuming no-tension material, since little tensile strength is observed in masonry material, with linear stress-strain relationship in compression, the curvature of an element depends on whether its cross-section is uncracked or partially cracked. As it is well known, if the compressive force acting on a section made of a tensionless material is within the kern (core) of the section, the section will remain uncracked; in the opposite case it will be partially cracked. Writing the equilibrium of the jth cross section for these two different conditions, for the (j+1)th element the following expression of dimensionless curvature can be obtained

$$\phi_{j+1} D = \frac{N_j}{BDE}\lambda_j \quad (4)$$

Where N_j is the resultant compressive force acting on the jth cross section with the eccentricity e_j, E is the elastic modulus of masonry and λ_j is a parameter given as

$$\lambda_j = \begin{cases} 12(e_j/D) & \text{for } 0 \le e_j/D \le 1/6 \\ \dfrac{2}{9\left(1/2 - e_j/D\right)^2} & \text{for } 1/6 \le e_j/D < 1/2 \end{cases} \quad (5)$$

(j = 0, 1, 2, ..., n-1)

The resultant compressive force and flexural moment acting on the jth cross section can be expressed respectively by

$$N_j = j\frac{W}{n} \quad (6a)$$

$$M_j = \frac{W}{n}\sum_{i=1}^{j}\left(y_j - y_{Gi}\right) + c\frac{H}{n}\frac{W}{n}\frac{1}{(n-1/2)}\sum_{i=1}^{j}(n-i+1/2)(j-i+1/2) \quad (6b)$$

Considering that the summation of $\sum_{i=1}^{j} i$ is equal to $j(j+1)/2$, the ratio between the quantities on the right-hand side of Equations (6a) and (6b) yields the eccentricity in the dimensionless form as

$$\frac{e_j}{D} = \frac{y_j}{D} - \frac{1}{j}\sum_{i=1}^{j}\frac{y_{Gi}}{D} + c\xi\frac{1}{j(n-1/2)}\sum_{i=1}^{j}(n-i+1/2)(j-i+1/2) \quad (j = 0, 1, ..., n) \quad (7)$$

For the top cross section, j = 0, of the pier, this expression gives $e_0/D = y_0/D = 0$, because the second term, that is, the first summation on the right-hand side of Equation (7) is equal to zero for j = 0.

The coordinate y of the centre of gravity of the jth element, Figure 6, can be obtained by the same procedure as for the coordinate y_j of the centroid of the jth cross-section. In the dimensionless form, the following expression can easily be deduced (La Mendola et al., 1995).

$$\frac{y_{Gj}}{D} = \frac{y_{j-1}}{D} + \frac{1}{2}\xi\beta + \frac{3}{8}\xi^2\phi_j D - \frac{1}{2}\sum_{i=1}^{j}\xi^2\phi_i D \quad (8)$$

(j = 1, 2, ..., n)

Substitution of Equation (6a) into Equation (4) yields the dimensionless curvature of the (j+1)th element in the form

$$\phi_{j+1} D = \frac{\gamma D}{E}\xi j\lambda_j \quad (9)$$

(j = 0, 1, 2, ..., n-1)

Where $\gamma = W/(BDH)$ is the weight per unit of volume of the pier.

COMPUTATIONAL PROCEDURE

For any pier from the highest part of the aqueduct, the whole $c-\delta$ curve and c_{max} can be determined by using Equations (7), (5), (9), (3) and (8) in order. For this purpose, the pier is divided ideally into sufficiently high number of elements, hence, discretization parameter ξ becomes known. The calculations performed have shown that the values such as 0.20 and 0.25 are appropriate for the ξ. Bigger values of this parameter may cause misleading or wrong results. Assigning a small value of c, and taking a trial value of the top rotation β, using Equation (7) and then Equations (5) and (9) for j = 0, one obtains $\phi_1 D = 0$; therefore Equation (3) gives the $y_1/D = \xi\beta$. Then, using the equations just mentioned in the same order but for j = 1, one obtains y_2/D, and so on (La Mendola et al., 1995). When the index j reaches the value n-1 in Equation (9), the following convergence criterion which implies zero rotation at the base (fixed end) of the pier, is controlled

$$\beta = \sum_{i=1}^{n}\alpha_i = \sum_{i=1}^{n}\xi\phi_i D \quad (10)$$

It is repeated with a decreased value of β, if $\beta - \sum_{i=1}^{n}\xi\phi_i D > 0$, and an increased value of β is used in the opposite case. It must be

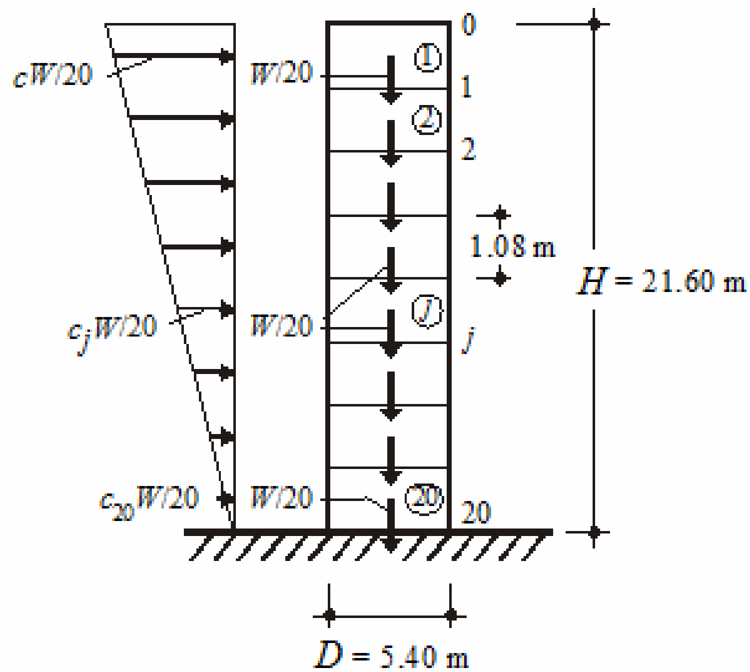

Figure 7. The most slender pier of the aqueduct.

expressed that a reasonably small tolerance value (0.00005 radians) is chosen to stop the procedure. When convergence on β is reached, in other words, after the actual value of this rotation corresponding to the assigned value of c is determined iteratively, the deflection $y_n = \delta$ can be calculated directly from Equation (3) (La Mendola et al., 1995). Repeating the procedure with variation in β and increasing this quantity gradually, the whole curve c versus δ can be drawn and hence c_{max}, that represents maximum out-of-plane inertia force to which pier can resist, can be determined. The maximum value of β consistent with the equilibrium of the pier corresponds to the limit condition at which the dimensionless eccentricity at the base cross section is equal to 1/2. The resultant out-of-plane inertia force, F, at any loading step can be computed by

$$F = \sum_{j=1}^{n} f_j = \sum_{j=1}^{n} c[(n-j+1/2)/(n-1/2)]\frac{W}{n} \tag{11}$$

Utilising this expression and using previously obtained δ values the whole force – displacement, $F - \delta$, curve can also be obtained. To implement the calculations, a computer program in C++, named OSAFA (Out-of-plane Seismic Analysis for Aqueducts), was developed by the authors.

NUMERICAL RESULTS AND DISCUSSION

The preceding procedure is now applied to obtain the whole $c - \delta$, $F - \delta$ curves and c_{max}, F_{max} values for a typical pier of the highest part of the aqueduct. In this part the aqueduct has a depth between ~ 5.00 – 5.65 m and has an average height of ~ 21.40 – 21.80 m. Width of the piers differed from each other. Almost the whole structure is made of stone (limestone, Kufeki Stone) which has a weight per unit of volume of 26.5 kN/m^3 and elastic modulus ~ 5000 Mpa (Yorulmaz and Celik, 1995). Thus, for the considered pier, Figure 7, the following data are taken: H = 21.60 m, D = 5.40 m, B = 3.50 m (but, in the analysis the value of B is taken as 1 m, because there is not any effect of B on the results), γ = 26.5 kN/m^3, E = 5000 MPa. Consequently, the pier has $\gamma D/E = 2.862 \times 10^{-5}$, Equation (9), and slenderness ratio H/D = 4. It is ideally divided into 20 elements, Figure 7, so that the discretization parameter ξ is 0.20.

The results of the analysis are shown in Figures 8a and b as $c - \delta$ and $F - \delta$ curves, respectively. Key features of the out-of-plane response of the pier can be traced from the curves in these figures. For example, referring to $c - \delta$ curve, Figure 8a, the following features are observed. Initially, the pier behaves as a linear-elastic element. Then, with the formation of first crack, when the seismic coefficient reaches approximately 0.175, it begins to behave in a non-linear manner. The pier continues resisting out-of-plane loads beyond initial cracking, but loses lateral stiffness as this first crack grows and new cracks are formed. Eventually, at the end of inelastic range, the seismic coefficient attains its maximum value c_{max} = 0.34 producing the deflection δ_{max} = 23.80 cm. In this limit state, the dimensionless eccentricity at the base of the pier is e_{20}/D = 0.484. It should be clarified that, from the formation of first crack to the maximum lateral resistance, the pier is stable horizontally. But, after the peak, when the dimensionless eccentricity at the base section of the pier reaches the limit value of 0.5, that is,

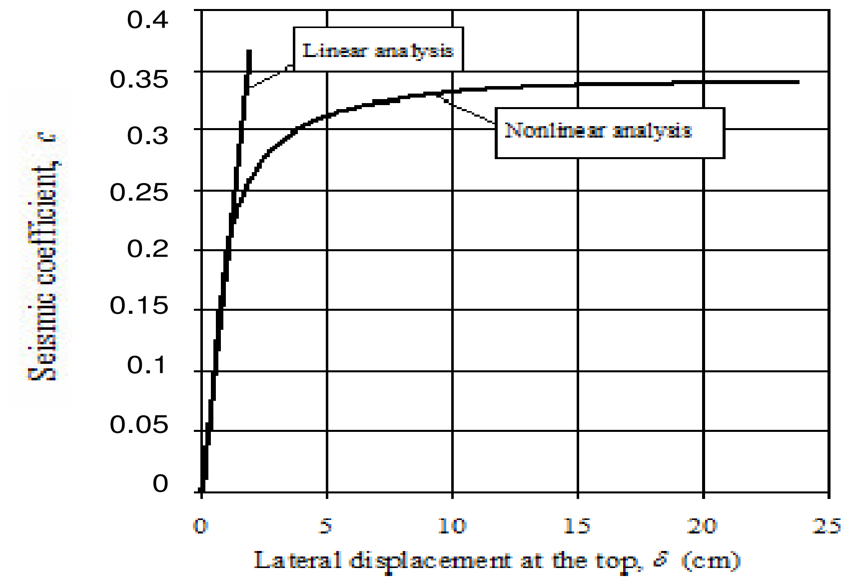

(a)

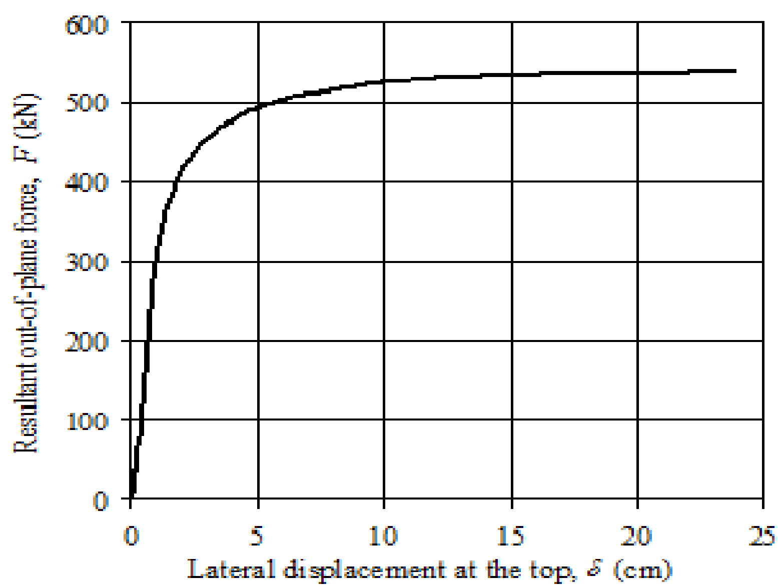

(b)

Figure 8. Resistance of the most slender part of the aqueduct against out-of-plane seismic forces: (a) $c - \delta$ curve, (b) $F - \delta$ curve.

when the resultant of all forces falls outside the base, the pier loses its horizontal stability and goes to the overturning regime. In Figure 8a, the response obtained with linear analysis considering the material of the pier has unlimited tensile strength as well as infinite compressive strength is also shown. The value of maximum seismic coefficient evaluated by this analysis is $c_{max,lin}$ = 0.366, thus, there is about 8% difference between non-linear and linear analyses. It should be stressed that the reduction in seismic coefficient with respect to linear analysis almost solely because of the nonlinearity of the moment – curvature law, due to the no-tension material assumption.

From Equation 11 resultant out-of-plane inertia force corresponding to c_{max} is obtained as $F_{max} = c_{max}W/1.95$. On the other hand, with a single-degree-of-freedom approximation for the pier, maximum lateral force, F_0, at the threshold of overturning as determined from simple

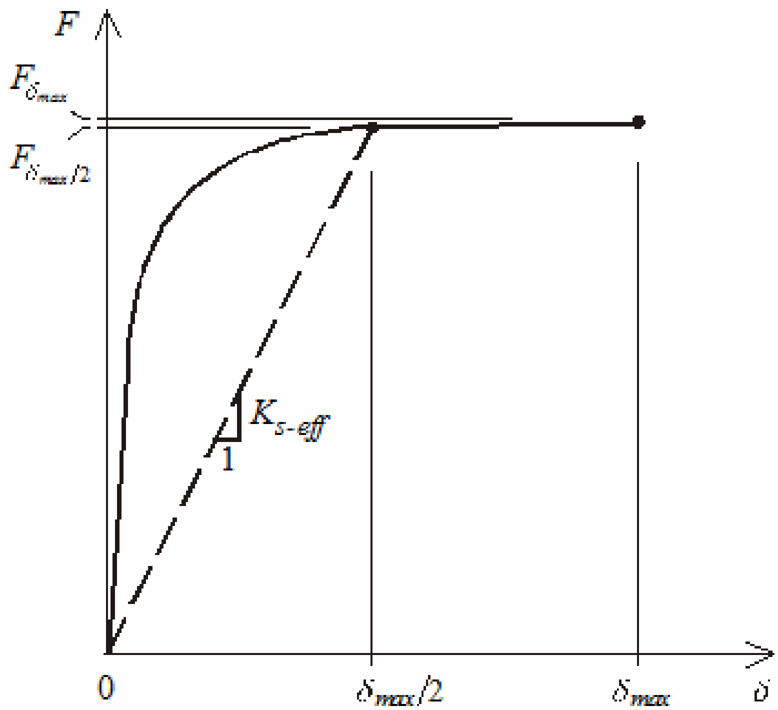

Figure 9. Effective secant stiffness, $K_{s\text{-}eff}$, of substitute structure.

statics is given by Equation 12

$$F_0 = M_e a_0 \tag{12}$$

Where M_e is the effective mass of the pier and a_0 is the overturning acceleration. The effective mass can be calculated using the following equation (Doherty et al., 2002)

$$M_e = \frac{\left(\sum_{j=1}^{20} m_j \Delta_j\right)^2}{\sum_{j=1}^{20} m_j \Delta_j^2} \tag{13}$$

Where m_j and Δ_j are the mass and displacement of the jth element, respectively. For the considered pier with uniformly distributed mass, the effective mass has been calculated as $M_e = 3M/4$, where M is the total mass of the pier. It must be noted that this value of M_e is based on the assumption of a triangular shaped relative displacement profile. Using this value of M_e in Equation 12 and then equating this equation to F_{max}, the value of overturning acceleration is obtained $a_0 = c_{max}g/(1.95 \times 0.75) = 0.23$ g, where g is the acceleration of gravity. Although, this result is a good indication for resistance and implies that the aqueduct is neither dangerously weak nor strong against out-of-plane seismic forces, for a more comprehensive understanding of the behaviour of the structure, the stiffness and period characteristics should also be investigated. As known, in earthquake response the relationship between structural and excitation periods is also significant.

The traditional method of selecting secant stiffness for use with a single-degree-of-freedom representation of a multi-degree-of-freedom system is not straightforward for non-ductile systems such as unreinforced masonry (Doherty et al., 2002). For unreinforced masonry, the effective secant stiffness covering the entire range of displacement, from $\delta = 0$ to $\delta = \delta_{max}$ can be defined from the system's non-linear force-displacement response curve, as the secant stiffness at $\delta = \delta_{max}/2$ (Doherty et al., 2002), Figure 9, and expressed mathematically by

$$K_{s\text{-}eff} = F_{\delta max/2} \,/\, (\delta_{max}/2) \tag{14}$$

Then, the effective undamped natural period, $T_{s\text{-}eff}$, for the equivalent single-degree-of-freedom system is accordingly given by the following equation

$$T_{s-eff} = 2\pi / \sqrt{K_{s-eff} / M_e} \tag{15}$$

For the considered pier, taking $\delta_{max}/2$ and $F_{\delta max/2}$ values from Figure 8b, then using Equations 14 and 15 in order, $T_{s\text{-}eff}$ is obtained as 1.45 s. According to this result and previously obtained overturning acceleration value, it can be said that the aqueduct can survive out-of-plane earthquake ground motions of moderate magnitude and usually encountered periods, whereas it is vulnerable to the ones containing long-period pulses, since, it is obvious that this type of excitations can cause resonance in the structure.

A more detailed investigation of the out-of-plane seismic behaviour of the aqueduct can be made with a non-linear time-history analysis procedure. Such an analysis requires selection or construction of appropriate earthquake ground motion records for the site and determination of the damping characteristics of the structure. Earthquake ground motions can be obtained by utilising various computer programs which provide simulated time-history of the ground acceleration, once the maximum ground acceleration and other relevant characteristics of the site are given as input. On the other hand, the determination of exact damping properties of the structure is a difficult task. Determination of the damping properties of the structure and a time-history analysis implementation exceeds the scope of this paper.

Conclusions

The protection of historical and cultural heritage is a social responsibility. The structural assessment of this heritage has a special importance as being the very first step of the engineering interventions. In this work, using an efficient numerical model that takes into account the cracking of the sections and the second-order effects, out-of-plane seismic resistance of the Bozdogan aqueduct in Istanbul is investigated. One pier of the most slender part of this stone masonry structure is modelled as a prismatic vertical cantilever undergoing static lateral loading having inverted triangular shape and rising intensity. Since the masonry material cracks when the loading on the pier is increased, the problem is non-linear. The main conclusions drawn from the analysis can be summarised as:

1. Although with a high probability it was designed and built with little or no regard for the effects of seismic loading, the aqueduct has a moderate resistance against out-of-plane seismic forces.
2. The aqueduct can withstand out-of-plane earthquake ground motions of medium size and mostly encountered periods, but it is vulnerable to the ones containing long-period pulses.
3. Obtained results are for the most slender part of the aqueduct. Since the other parts of the structure have different geometrical and vibrational characteristics, it is obvious that, those parts will have different levels of out-of-plane seismic resistance.
4. Following the principles of strengthening and restoration of historical structures, appropriate strengthening measures should be taken to protect the aqueduct against out-of-plane earthquake ground motions with long periods.
5. The developed procedure and computer program can be useful in the seismic analysis of similar masonry structures.

NOMENCLATURE

The following symbols are used in this paper:

a_0: overturning acceleration, B: width of pier, c:seismic coefficient , D: depth of pier, F: resultant lateral seismic force, f:lateral seismic loading, H:height of the pier, E:modulus of elasticity, e: eccentricity, K: secant stiffness, M: bending moment; total mass of the pier, M_e: effective mass, m: mass of an element, N: axial force, n: number of elements, $O(x,y)$: system of coordinates, r: radius of curvature, W: weight of the pier, T: natural period, α:angle (for jth element $\alpha_j = H_e/r_j$), β:rotation of top cross-section, δ:deflection of the top cross-section of the pier, Δ: displacement of the element, ξ:discretization parameter, γ: weight of the unit volume of the pier, ϕ: curvature of the element.

REFERENCES

Akinci S (1992). The restoration of the Bozdogan (Valens) Aqueduct in Istanbul. Yapı, 124: 69-75 (in Turkish).

Ambraseys NN, Finkel CF (1990). The Marmara Sea earthquake of 1509. Terra Nova, 2: 167-174.

Ambraseys NN, Finkel CF (1995). The seismicity of Turkey and adjacent areas: a historical review. Eren Ltd., Istanbul.

Barka A (2000). Earthquake risk in Marmara, Proceedings of Second "Istanbul and Earthquake" Symposium. Chamber of Turkish Civil Engineers, Istanbul, 27: 5-15 (in Turkish).

Bruneau M, Lamontagne M (1994). Damage from 20th century earthquakes in eastern Canada and seismic vulnerability of unreinforced masonry buildings. Canadian J. Civil Eng., 21: 643-662.

Casolo S (2000). Modelling the out-of-plane seismic behaviour of masonry walls by rigid elements. Earthquake Eng. Struct. Dynamics, 29: 1797-1813.

Cecen K (1996). Sinan's water supply system in Istanbul. General Directorate of Istanbul Water and Sewerage Administration, Istanbul.

De Felice G, Giannini R (2001). Out-of-plane seismic resistance of masonry walls. Journal of Earthquake Engineering, 5(2): 253-271.

Doherty K, Griffith MC, Lam N, Wilson J (2002). Displacement-based seismic analysis for out-of-plane bending of unreinforced masonry walls. Earthquake Engineering and Structural Dynamics, 31: 833-850.

Eyice S (1992). Encyclopedia of Islam. Publication of Turkish Religious Foundation, Istanbul (in Turkish).

Eyidogan H (2000). Seismicity of Marmara and Istanbul, Proceedings of Second "Istanbul and Earthquake" Symposium. Chamber of Turkish Civil Engineers, Istanbul, s. 17-23 (in Turkish).

Fardis M (1995). Lessons learnt in past earthquakes. Proceedings of 10th European Conference on Earthquake Engineering. Rotterdam, 779-788.

Kirimtayif S (2001). Converted Byzantine Churches in Istanbul. Ege Publication, Istanbul.

La Mendola L, Papia M (1993). Stability of masonry piers under their own weight and eccentric load. J. Struct. Eng. ASCE, 119(6): 1678-1693.

La Mendola L, Papia M, Zingone G (1995). Stability of masonry walls subjected to seismic transverse forces. J. Struct. Eng. ASCE, 121(11): 1581-1587.

Panoramio (2009) web site: http://www.panoramio.com/photo/6523562

Paulay T, Priestly MJN (1992). Seismic Design of Reinforced Concrete and Masonry Buildings. John Wiley and Sons, Inc. USA.

Pegon P, Pinto AV, Geradin M (2001). Numerical modelling of stone-block monumental structures. Comput. Struct., 79: 2165-2181.

TCF (2009). Turkish Cultural Foundation, Water supply systems: aqueducts built in Istanbul, web site: http://www.turkishculture.org/pages.php?ParentID=6&ID=102.

Wikimedia (2009). web site: http://commons.wikimedia.org/wiki/File:Segovia_Aqueduct.JPG.

Yorulmaz M, Celik OC (1995). Structural analysis of the Bozdogan (Valens) Aqueduct in Istanbul. Arch Bridges. Thomas Telford, London, pp. 175-180.